

Graphical Models for Skin Detection [★]

Huicheng Zheng¹, Mohamed Daoudi², and Bruno Jedynak³

¹ MIIRE Group LIFL (UMR 8022)
Rue G. Marconi Cité scientifique
59655 Villeneuve d'Ascq, France
`zheng@enic.fr`

² Laboratoire d'Informatique (EA 2101)
Université François-Rabelais
64 avenue Jean Portalis, Tours
`mohamed.daoudi@univ-tours.fr`

³ Center for Imaging Science
The Johns Hopkins University
3400 North Charles Street
Baltimore, MD 21218-2686, U.S.A
`bruno.jedynak@jhu.edu`

Abstract. We construct two graphical models for skin detection from a large collection of labeled data. Within it, parameter estimation is eradicated by tree approximations and the belief propagation algorithm permits to obtain exact and fast solution for skin probability at pixel locations. We then assess the performance on the Compaq database.

1 Introduction

1.1 Skin Detection

Skin detection consists in detecting human skin pixels from an image. It plays an important role in various applications such as face detection [4], searching and filtering image content on the web [5][8]. Research has been performed on the detection of human skin pixels in color images by using various skin color models such as Gaussian, Gaussian mixture or histograms [2]. A Bayesian network approach for skin detection has been proposed by [3].

We have in our hands the publicly available Compaq Database [2] with more than ten thousand images. Skin pixels are manually labeled for each image. We shall infer a model from this data in order to perform skin detection on new images.

The rest of the paper is organized as follows: in Section 2, we detail graphical models for skin detection. Section 3 is devoted to experiments and comparisons with alternative methods. Finally, the conclusion is in Section 4.

[★] This work was partially supported by CNRS under MathStic Project

2 Graphical Models

2.1 Notations

Let us fix the notations. The set of pixels of an image is S . The color of a pixel $s \in S$ is x_s . It is a three dimensional random variable, each component being coded on one octet. $C = \{0, \dots, 255\}^3$ denotes the RGB color space. The “skinness” of a pixel s , is y_s with $y_s = 1$ if s is a skin pixel and $y_s = 0$ if not. The color image, which is the vector of color pixels, is denoted by x and the binary image made up of the y_s ’s is denoted by y .

Let us assume for a moment that we knew the joint probability distribution $p(x, y)$ of the vector (x, y) , then Bayesian analysis tells us that, whatever cost function the user might think of, all that is needed is the posterior distribution $p(y|x)$.

Inference problems can often be guided by graphical models, in which we represent variables and their relationship with nodes/vertices and edges. Inference on graphical models are implemented in many disciplines like AI, computer vision, statistical physics and error-correcting coding theory [7], thus it is not surprising to see many variants of graphical models. In the following we shall introduce the pairwise Markov random fields (MRFs) used in our work.

2.2 Pairwise Markov Random Fields

Pairwise MRFs provide attractive theoretical models for computer vision problems such as image segmentation or image restoration [1]. They are undirected graphs in which there exist only pairwise relationship between nodes. There is no causal node in such graphs like those in the Bayesian networks where there are causal nodes called “parents” of other nodes. Pairwise MRFs are the simplest and most used MRFs in computer vision.

We propose two graphical models called hidden Markov model (HMM) and first-order model (FOM) for skin detection. They are shown in Fig. 1 for a lattice of 4×4 . The label image y is the hidden layer with nodes y_s represented by empty circles. The color image x is the observed layer with nodes x_s represented by filled-in circles. The links between neighboring nodes represent the potential functions of the corresponding nodes. HMM is a special case of FOM.

The distribution of the FOM is then:

$$\pi(x) = \frac{1}{Z} \prod_{s \sim t} \psi_{st}(x_s, x_t, y_s, y_t) \quad (1)$$

where Z is a normalizing function and ψ_{st} are parameters to estimate from the data. Parameter estimation for FOM is hard since $\psi_{st}(x_s, x_t, y_s, y_t)$ involve a huge parameter space.

Let us assume for now that the graph of pixels was a tree. Then the distribution of FOM could be written as:

$$p(y|x) \propto \prod_{s \sim t} \frac{p(x_s, x_t, y_s, y_t)}{p(x_s, y_s)p(x_t, y_t)} \prod_{s \in S} p(x_s, y_s) \quad (2)$$

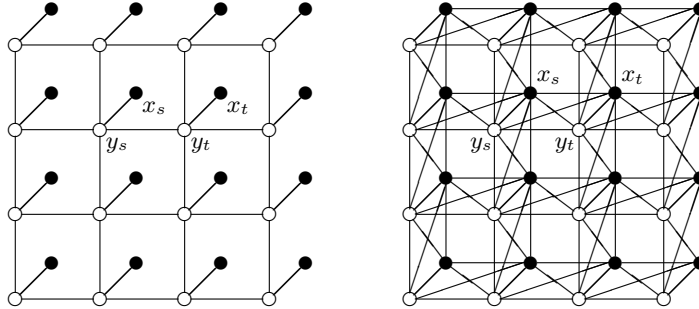


Fig. 1. Left: Graphical models of HMM. **Right:** Graphical models of FOM. The label image y is composed of empty circles. The color image x is represented by the filled-in circles. These models are pairwise in terms of pixel lattice

The \propto in the above equations means equality up to a normalization function that might depend on x but not on y . The parameters can be empirically estimated from the data. This model is referred to as TFOM for Tree First-Order Model.

In the case of HMM, the distribution boils down to:

$$p(y|x) \propto \prod_{s \sim t} \frac{p(y_s, y_t)}{p(y_s)p(y_t)} \prod_{s \in S} p(x_s, y_s) \quad (3)$$

It will be referred to as THMM for Tree Hidden Markov Model.

3 Experiments

The Compaq database is split into two almost equal parts, the training set and the test set, randomly. Belief propagation algorithm [7] is implemented for probability inference of THMM and TFOM at pixel locations. Each graph has been approximated by Bethe Tree Approximation [6]. We refer to the independent model in [2] as the baseline model and compare THMM and TFOM with this model.

4 Summary and Conclusions

We have derived several graphical models for skin detection that perform uniformly better than the baseline model. All the models in this paper are pixel-based. In our future work, we can try to combine the pixel-based techniques with shape-based segmentation.

References

1. S. Geman and D. Geman. Stochastic relaxation, gibbs distributions, and the bayesian restoration of images. *IEEE Transactions on PAMI*, 6:721–741, 1984.

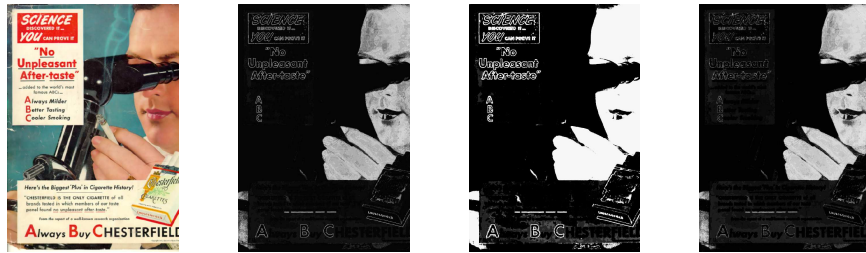


Fig. 2. **First:** original color image. **Second:** result for the Baseline model. **Third:** result for the THMM model. **Last:** result for the TFOM model

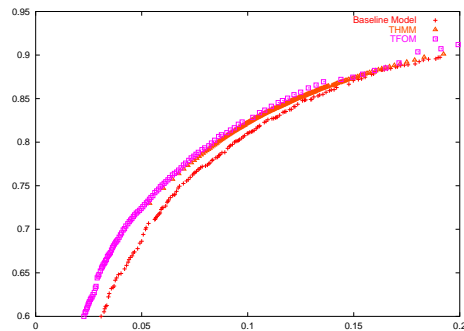


Fig. 3. Receiver Operating Characteristics (ROC) curve for each model. x-axis is the false positive rate, y-axis is the detection rate. Baseline model is shown with crosses, THMM with triangles, while TFOM with squares.

2. M. Jones and J. M. Rehg. Statistical color models with application to skin detection. In *Computer Vision and Pattern Recognition*, pages 274–280, 1999.
3. N. Sebe, I. Cohen, T. S. Huang, and T. Gevers. Skin detection : A bayesian network approach. In *Proceedings of International Conference on Pattern Recognition*, volume 2, pages 903–906, August 2004.
4. J.-C. Terrillon, M. N. Shirazi, H. Fukamachi, and S. Akamatsu. Comparative performance of different skin chrominance models and chrominance spaces for the automatic detection of human faces in color images. In *Fourth International Conference On Automatic Face and gesture Recognition*, pages 54–61, 2000.
5. J. Z. Wang, J. Li, G. Wiederhold, and O. Firschein. Classifying objectionable websites based on image content. *Notes in Computer Science, Special issue on interactive distributed multimedia systems and telecommunication services*, 21/15:113–124, 1998.
6. C. Wu and P. C. Doerschuk. Tree approximations to markov random fields. *IEEE Transactions on PAMI*, 17(4):391–402, April 1995.
7. J. S. Yedidia, W. T. Freeman, and Y. Weiss. Understanding belief propagation and its generalisations. Technical Report TR-2001-22, Mitsubishi Research Laboratories, January 2002.
8. H. Zheng, M. Daoudi, and B. Jedynek. Blocking adult images based on statistical skin. *Electronic Letters on Computer Vision and Image Analysis*, 4(2):1–14, Decembre 2004.